International Journal of Sediment Research 33 (2018) 35–46

Contents lists available at ScienceDirect

International Journal of Sediment Research

journal homepage: www.elsevier.com/locate/ijsrc

Original Research

Application of an impact plate – Bedload transport measuring system for high-speed flows

Takahiro Koshiba [a], Christian Auel [b], Daizo Tsutsumi [c], Sameh A. Kantoush [a], Tetsuya Sumi [a,*]

[a] Water Resources Research Center, Disaster Prevention Research Institute, Kyoto University, Goka-sho, Uji 611-0011, Japan
[b] ILF Consulting Engineers, Feldkreuzstrasse 3, 6063 Rum/Innsbruck, Austria
[c] Hodaka Sedimentation Observatory, Research Center for Fluvial and Coastal Disasters, Disaster Prevention Research Institute, Kyoto University, Gifu 506-1422, Japan

ARTICLE INFO

Article history:
Received 1 September 2016
Received in revised form
27 November 2017
Accepted 18 December 2017
Available online 26 December 2017

Keywords:
Sediment Bypass Tunnel
Bedload
Acoustic measurement
Geophone
Hydrophone
High-speed flow

ABSTRACT

To achieve the sustainable use of dams, the development of methods for sediment management in reservoirs is required. One such method includes the use of Sediment Bypass Tunnels (SBTs) to divert sediment around a dam, thereby preventing sedimentation in the reservoir. However, SBTs are prone to severe invert abrasion caused by the high sediment flux. Therefore, it is necessary to establish a measurement system of the sediment transport rate in these tunnels. One system to measure sediment transport in rivers is the Swiss plate geophone, which can register plate vibrations caused by particle impact. In Japan, the Japanese pipe microphone is used, and sediment transport is measured based on the sound emitted by the particle impact. In this study an attempt was made to optimize the advantages of both systems by fixing a microphone and an acceleration sensor to a steel plate. The results of calibration experiments with this new system are presented and compared with the existing methods. It was found that the acceleration sensor can detect sediment particles larger than 2 mm in diameter. Moreover, a new parameter, referred to as the detection rate, was introduced to describe the correlation between the actual amount of sediment and the registered output. Finally, two parameters - the saturation rate and hit rate - are introduced and exhibit strong correlation with the detection rate.

1. Introduction

Many dams throughout the world are prone to reservoir sedimentation and require sedimentation management. An advanced technique applied to address this issue is the use of sediment bypass tunnels (SBTs), which are implemented to reduce suspended load and bedload deposition in reservoirs by routing the incoming sediment around the dam (Auel & Boes, 2011b; Sumi et al., 2004). The use of SBTs, which can redistribute approximately 77 to 94% of incoming sediment, is an effective strategy (Auel et al., 2016b). However, measuring and quantifying the sediment transport in an SBT is a challenging research subject (e.g., Hagmann et al., 2015). In particular, invert abrasion is a severe problem faced by most SBTs, as it increases maintenance costs (Auel & Boes, 2011a; Baumer & Radogna, 2015; Jacobs & Hagmann, 2015; Nakajima et al., 2015). Invert abrasion is caused by a combination of high flow velocities and high sediment transport rates (Auel, 2014). Sediment transport, which is ideally routed downstream of a dam during floods, should be considered for comprehensive river basin management and is also important regarding environmental aspects of dam operation, as morphologic variability is enhanced (Auel et al., 2017b; Facchini et al., 2015). Various techniques have been developed to monitor suspended sediment, such as utilizing turbidity current meters (Kantoush et al., 2011). However, a limited number of techniques for field observation of bedload sediment transport are available to understand the associated mechanisms and quantify the bedload transport rates (BTRs).

As a direct BTR measuring system, sediment samplers have been used for decades (Bunte et al., 2004; Helley & Smith, 1971; Reid et al., 1980). Nevertheless, despite the high reliability of the sampling systems, their disadvantages include their time-consuming and laborious nature and their ineffectiveness under

* Corresponding author.
E-mail addresses: koshiba.takahiro.47v@st.kyoto-u.ac.jp (T. Koshiba), christian.auel@alumni.ethz.ch (C. Auel), tsutsumi.daizo.8m@kyoto-u.ac.jp (D. Tsutsumi), kantoush.samehahmed.2n@kyoto-u.ac.jp (S.A. Kantoush), sumi.tetsuya.2s@kyoto-u.ac.jp (T. Sumi).

https://doi.org/10.1016/j.ijsrc.2017.12.003
1001-6279/

Nomenclature

A_{max}	maximum amplitude within each run [V]
B	plate length [mm]
D_s	grain size [mm]
Fr	Froude number [dimensionless]
h	flow depth [m]
I_{ps}	number of impulses measured by the microphone [dimensionless]
I_{pv}	number of impulses measured by the acceleration sensor [dimensionless]
L_p	jump length [m]
P_n	number of particles fed in each run [dimensionless]
$P(L_p)$	hit rate [dimensionless]
Q	flow discharge [m^3/s]
R_s	saturation rate [dimensionless]
R_d	detection rate [dimensionless]
Re	Reynolds number [dimensionless]
S_p	average value of voltage measured by the microphone [mV]
T	duration of single particle raw data of the signal [s]
V	flow velocity [m/s]
V_p	average value of the acceleration sensor signal [mV]
W	sediment weight [g]
Δt	impact time of one particle hitting the plate [s]
θ	Shields' parameter [dimensionless]
θ_c	critical Shields' parameter [dimensionless]
ν	kinematic viscosity [m^2/s]

conditions of high flow velocity and transportation of coarse sediment, which hinder them from being deployed in SBTs, where the maximum water velocity reaches 10 m/s and a wide diameter range of transported gravel prevails (Auel, 2014).

To overcome the inconvenience of samplers, recent studies have attempted to collect indirect bedload transport observations by developing different bedload surrogate monitoring techniques (Gray et al., 2010; Mizuyama et al., 2010a; Rickenmann & McArdell, 2007; Taniguchi et al., 1992). These techniques involve the use of microphones, acceleration sensors, and geophones placed on a steel plate or a hollow steel pipe. Subsequently, they record acoustic or acceleration data generated by particles as they collide with each other, which are used to measure the bedload transportation properties. These surrogate monitoring systems yield continuous bedload monitoring, and previous applications have covered a wide range of riverbed conditions.

The Swiss impact plate geophone (hereafter termed SPG) was developed in the early 1980s by a Swiss research group at the Swiss Federal Institute for Forest, Snow and Landscape Research (WSL) and the Laboratory of Hydraulics, Hydrology and Glaciology, Swiss Federal Institute of Technology (VAW). The SPG consists of a 50 cm by 36 cm steel plate with a geophone sensor (Geospace GS-20DX, manufactured by Geospace Technologies, Houston, TX) mounted underneath. The sensor is embedded in a steel frame and installed directly in a riverbed. A similar impact sensor, consisting of a metal plate with an accelerometer, has also been demonstrated to work effectively (Reid et al., 2007; Tsakiris et al., 2014). It is also recommended to make observations using two or more sensors to gain detailed information on bedload transport (Beylich & Laute, 2014; Mao et al., 2016). Recently, validation studies of bedload surrogate monitoring systems in flume experiments have been done, suggesting their usefulness for field observations in natural rivers. Numerous studies have been summarized in several recent reviews (Gray et al., 2010; Rickenmann, 2017b).

In particular, the SPG has been extensively used in European countries, especially in the mountainous areas of Switzerland, Austria, and Italy (Rickenmann, 2017a; Rickenmann et al., 2014). The SPG estimates the BTRs based on the plate vibration caused by passing sediment and recorded by the geophone sensor. At the Erlenbach Stream in Switzerland, field observations were done, and a high correlation between long-term BTRs and the SPG output was confirmed (Rickenmann et al., 2012). Furthermore, the SPG is resistant to the impact of sediment; therefore, installation of an SPG on the invert of an SBT is feasible. An SPG system was installed in an SBT for the first time at the Solis dam and has been in operation since 2012 (Auel & Boes, 2011a; Hagmann et al., 2015). However, it has also been found that the SPG cannot detect fine sediments with diameters smaller than 1 to 2 cm (Rickenmann et al., 2012, 2014; Wyss et al., 2016a, 2016b). To clarify the effects of abrasion on the SBT invert, the grain size of the particles making contact is important, as the amount of abrasion on the invert not only depends on the sediment flux but also on the grain size (Auel, 2014).

In addition to the SPGs in Switzerland, another similar indirect BTR measuring system was developed and is widely used in Japan, namely, the Japanese pipe microphone (hereafter termed JPM) (Mizuyama et al., 2010a, 2010b). The JPM consists of a metal pipe installed directly in a riverbed. When gravel and sand particles pass over the pipe, the number of colliding particles is counted based on the number of impulses in the sound pressure over time. The JPM system is already installed in some rivers in Japan, e.g., the Yodagiri and Koshibu rivers, and bedload transport observation is done at the Hodaka Sedimentation Observatory, DPRI, Kyoto University (Tsutsumi et al., 2010). The studies at the observatory reveal that the JPM can detect sediment with a diameter larger than 2 mm. However, the JPM often underestimates the bedload when particle impacts are successive and overlap. Moreover, the pipe has a small dimension in the flow direction (pipe diameter of 48.6 mm), resulting in particles jumping over the pipe. Additionally, the JPM deforms easily when hit by large stones, which negatively affects the sound collection.

For BTR monitoring in SBTs, the grain size distribution of the transported sediment is important because grain size and the number of particles are required elements for calculating the amount of abrasion using Ishibashi's formula, which is widely used in Japan (Auel et al., 2016a; Ishibashi, 1983). Moreover, the installation costs should be limited for a surrogate bedload measurement system because the combination of multiple systems can realize a wide spatial bedload distribution in SBT, e.g., the cross-sectional bedload transport distribution. Therefore, an impact plate with a microphone has been selected for this study, considering both the robustness of plate-type systems and the JPM's ability to detect particles of $D_s > 2$ mm. Moreover, an acceleration sensor was mounted to the plate to compare the sensitivity with that of the microphone. The acceleration sensor is different from the traditional geophone sensor mounted on the SPG.

In this study, a series of flume experiments were done to calibrate the impact plate. The primary purpose was to investigate the basic characteristics of the impact plate, such as the minimal detectable particle size, the correlation between the bedload information, including the mass and the number of particles, and the impact plate's microphone or acceleration sensor response, i.e. the number of impulses and the average output voltage (introduced in Section 2). In particular, the number of impulses is promising and used to estimate the grain size for JPM analysis, e.g.,

Mao et al. (2016) successfully calibrated a JPM to observe transport rates for different classes of sediment coarser than 9 mm. In addition, the manner in which to address the expected difficulty of quantifying the bedload mass or particle number based on the aforementioned parameters, which was reported in past studies, is discussed (see also Mao et al., 2016; Mizuyama et al., 2010b; Wyss et al., 2016c).

2. Methods

2.1. Experimental setup

The experiments were done in a flume facility at the Laboratory of Hydraulics, Hydrology and Glaciology (VAW) of ETH Zurich, Switzerland. A series of experiments was done to measure the signals produced by particles colliding with the plate. The experimental setup consisted of an elevated water supply tank that discharges water through a jetbox (Schwalt & Hager, 1992) to a rectangular glass-sided flume with inner width, height, and length dimensions of 0.50, 0.60, and 9.00 m, respectively (Fig. 1). The jetbox enables regulation of the flow depth by vertically moving the opening. The flume bed was horizontal and fixed. The water flow was set to steady-state, supercritical conditions. The discharge was controlled using a gate valve, and a magnetic discharge meter was mounted inside the piping unit of the water supply pump. The flow velocity was obtained by dividing the discharge by the flow area, equal to the flume width times the flow depth, which was measured using a point gauge.

2.2. BTR measurement devices

The impact plate, manufactured by Hydrotech Co., Ltd. (Japan), was developed as an alternate surrogate BTR measurement system to overcome the disadvantages of the Japanese pipe microphone. The impact plate consists of a steel plate with the same dimensions as for the SPG system, a microphone, and an acceleration sensor. The same microphone model as for the Japanese pipe microphone system is mounted to the plate, and it registers microphone signals produced by the impact of sediment particles on the plate. The impact plate is expected to record the impact of small gravel particles with diameters of approximately 2 mm, which the JPM can detect, to ensure resistance to the impacts of coarse sediment. The detailed properties of the microphone can be found in the work of Taniguchi et al. (1992) and Goto et al. (2014).

Another sensor is the acceleration sensor, which has already been used for bedload monitoring in several studies (Beylich & Laute, 2014; Møen et al., 2010; Reid et al., 2007; Rickenmann, 2017a; Rickenmann et al., 2017; Tsakiris et al., 2014). The impact plate also includes an acceleration sensor (GH-313A, which serves as a sensor, and GA-223, which functions as a converter; manufactured by KEYENCE, Japan), which improves the measurement by recording data simultaneously with the microphone. This concept originated from an attempt to replace the SPG's geophone sensor with a sensor with a higher response frequency. It is likely that a sensor with a higher response frequency is more suitable for use on a rigid steel plate for detecting smaller grains

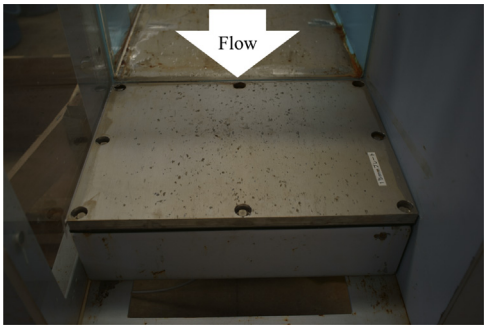

Fig. 2. Impact plate mounted below the steel plate in the test flume.

Fig. 3. Back side of the impact plate, the smaller sensor represents the acceleration sensor and the microphone is in the steel pipe (courtesy of Hydrotech Co., Ltd.).

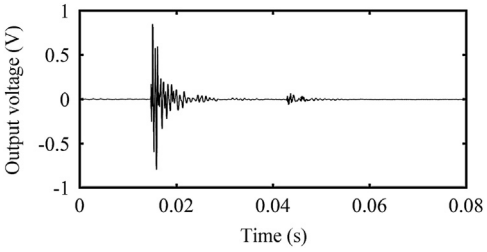

Fig. 4. Example of raw waveform data measured by the acceleration sensor when a single particle of $D_s = 50$ mm collides on the plate at $V = 4.5$ m/s.

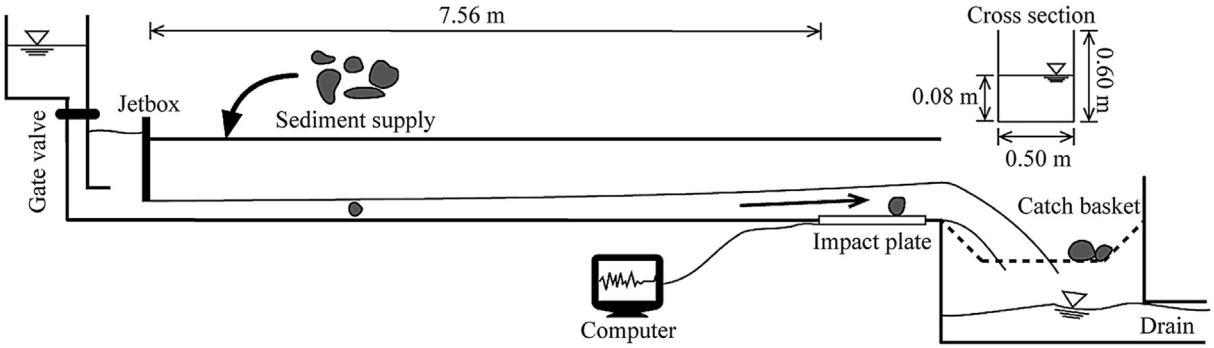

Fig. 1. Schematic view of the laboratory test flume.

Table 1
Experimental conditions (see notation list for definition of parameters).

	Flow					Sediment		
Case No.	Q [m^3/s]	V [m/s]	h [cm]	Fr [dimensionless]	Re [dimensionless]	D_s [mm]	W [g]	P_n [dimensionless]
1	0.10	2.5	8.0	2.82	610,000	2	50	3100
2	0.10	2.5	8.0	2.82	610,000	5	50	350
3	0.10	2.5	8.0	2.82	610,000	10	40	20
4	0.10	2.5	8.0	2.82	610,000	50	620	20
5	0.10	2.5	8.0	2.82	610,000	100	29376	20
6	0.18	4.5	8.0	5.08	1,090,000	2	50	3100
7	0.18	4.5	8.0	5.08	1,090,000	5	50	350
8	0.18	4.5	8.0	5.08	1,090,000	10	40	20
9	0.18	4.5	8.0	5.08	1,090,000	50	620	20
10	0.18	4.5	8.0	5.08	1,090,000	100	29376	20

Table 2
Dimensions of tested sediment.

Grain size D_s [mm]	b-axis [mm]	Average weight [g]
2	2.00–2.36	3.2 of 200 particles
5	5.00–6.00	14.3 of 100 particles
10	10.0–12.0	2.0
50	45.0–55.0	149.8
100	95.0–105.0	1468.8

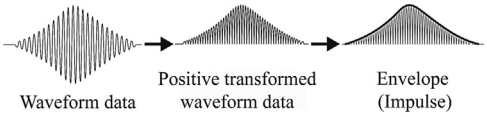

Fig. 5. Process of converting raw waveform data.

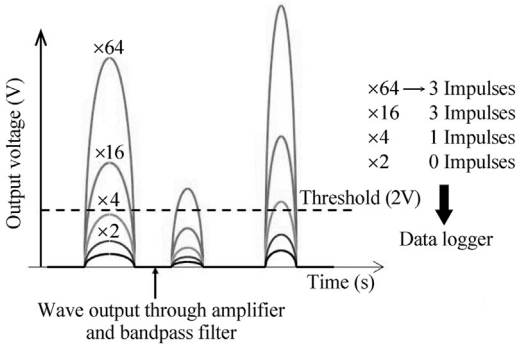

Fig. 6. Process to count the number of pulses.

than are detectable by a geophone sensor, which was designed for the observation of low-frequency seismic signals. The geophone sensor (20DX geophones) has a natural frequency of 10 Hz and flat response frequencies in the range of approximately 20–500 Hz, which are classified as ultralow frequencies (Roth et al., 2016; Wyss et al., 2016a). The frequency response of the replaced acceleration sensor is much higher, i.e., 0.1 to 80 kHz. Due to this difference, it might be expected that the acceleration sensor is more suitable than the geophone, especially for small bedload sediment fractions, because it has been reported that the dominant frequency of raw data of the signals produced by sediment impact increases as the sediment grain size decreases (Møen et al., 2010; Wyss et al., 2016a).

The impact plate consists of four parts: a steel plate, a microphone, an acceleration sensor, and a data logger. The steel plate is 49.2 cm in width, covering the whole flume width to allow all the test particles to pass over the plate, 35.8 cm in length in the flow direction and 1.5 cm in depth, being identical to the SPG (Rickenmann et al., 2014). The impact plate (shown in Fig. 2) was placed at the flume outlet, 7.56 m from the inlet (Fig. 1). The plate was affixed to the flume using four screws and acoustically isolated using a rubber material to minimize the detection of vibrations from the flume structure. Fig. 3 shows the downward facing side of the plate, where the smaller sensor represents the acceleration sensor and the microphone is connected to the steel pipe by a 90° angle pipe piece. The computer records the signals detected by the acceleration sensor and microphone sensor of the steel plate during each test with a sampling frequency of 50 kHz. The raw signal data were collected by both the microphone and the acceleration sensor at a rate of 50 kHz. Fig. 4 shows an example of the raw signal data recorded by the acceleration sensor when a single particle of $D_s = 50$ mm collides with the plate at $V = 4.5$ m/s.

2.3. Experimental conditions

A series of experiments was done to determine the behavior of the impact plate during particle impacts for various water velocities and grain sizes. The experimental conditions are listed in Table 1. The flow depth, h, was kept constant at 0.08 m, with the jetbox located at the entrance of the flume, whereas the water velocity was varied between two levels by controlling the flow discharge. Table 1 also lists five grain size fractions of gravel, which were tested in the experiment; the permutation of two flow velocities and five grain sizes yielded 10 different test cases. Each case was repeated 50 times; hence, 500 runs were made, although 12 runs were not recorded due to technical problems.

All gravel particles used in the experiments were sampled from a natural river, and, thus, had various shapes, including round, irregular, and angular shapes. The sediment was sieved in the laboratory to five uniform grain size fractions. Table 2 lists the mean particle size of each sieve fraction D_s, the sieve grid size (b-axis), and the average weight of each fraction. According to the average weight and D_s, the sediment particle density can be calculated as $\rho_s = 2700$ kg/m^3. The number of particles for each release, P_n, in Table 1 was calculated based on these parameters. Sediment particles were released into the test flume by hand just downstream of the jetbox. These gravel particles were transported along the flume, detected by the impact plate and captured using a basket. A constant sediment weight, W, of 50 g was used for two small grain sizes, i.e., $D_s = 2$ mm and 5 mm. For $D_s = 10$ mm, 50 mm, and 100 mm, a fixed number of 20 stones was added manually to the flow every five seconds.

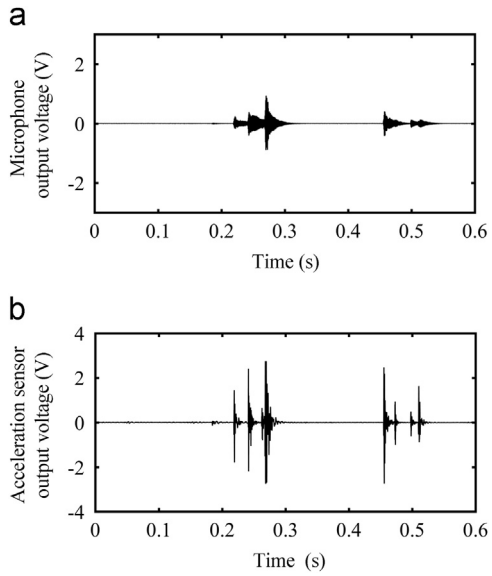

Fig. 7. Raw data of the signal waveform of case 10 (V = 4.5 m/s, D_s=100 mm, 20 particles) for a) the microphone, and b) the acceleration sensor.

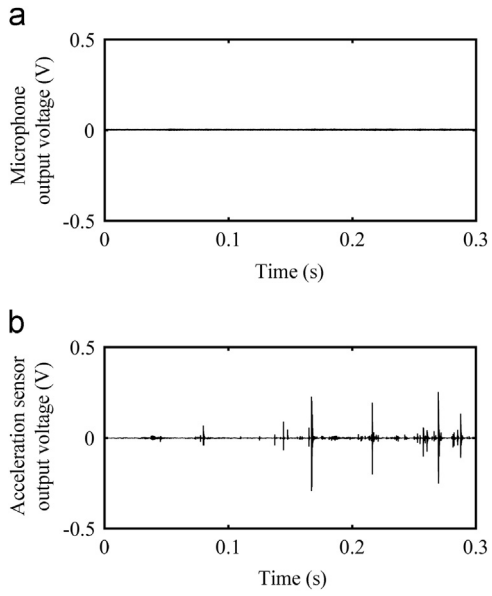

Fig. 8. Raw data of the signal waveform of case 6 (V = 4.5 m/s, D_s=2 mm, approximately 3100 particles) for a) the microphone, and b) the acceleration sensor.

2.4. Data processing

2.4.1. Microphone signal

In accordance with previous observations made using the JPM (Mizuyama et al., 2008; Suzuki et al., 2010), the following two parameters were calculated from the signal of the impact plate during each experiment: the number of impulses, I_{ps}, and the average value of the sound pressure, S_p. Both values were obtained via electronic processing of the analog signal in the data logger, and, thus, calculated simultaneously with the recording of the impact signals.

The recorded number of impulses I_{ps} represents the number of particles hitting the plate, and similar approaches are utilized not only for JPMs but also for SPG using a parameter called a packet (Wyss et al., 2016b). This approach significantly reduces the amount of data compared to collecting the raw data of the signal while keeping some information about the frequency and amplitude fractions of the signals produced by the particle impacts. To compute I_{ps}, the following steps were done using the data logger after the raw data of a signal was recorded. First, the raw data of the signal were amplified by a factor of 20 and sent through a band-path filter to extract a frequency of approximately 4.6 kHz, which was previously computed as the most effective frequency for distinguishing particle impacts on a plate by Hydrotech Co., Ltd. Subsequently, the filtered raw data of the signal were transformed into an absolute value since all the negative values were changed to positive ones (Fig. 5). An envelope curve was generated and amplified by a factor of 10 to accentuate the signals caused by particle impact. Then, the enveloped data were exported to 6 different channels in which the wave was amplified by a factor of 2, 4, 16, 64, 256, and 1024. Finally, the I_{ps} value for each amplification factor was defined as the number of impulses, which were counted for each envelope, exceeding a predefined threshold of 2 V (Fig. 6). The amplification scheme was originally developed to identify the best value to detect the highest number of particle impacts (Mizuyama et al., 2003).

Although I_{ps} is already commonly used with the JPM system to analyze field observations in Japan, it is also reported that I_{ps} can lead to underestimation of the number of particles because of the overlapping of single impulses when the sediment transport rate is high or when several gravel particles hit the plate simultaneously (Mizuyama et al., 2010a, 2010b). To address this shortcoming, the other summary value, obtained by using the enveloped data determined in the process of calculating I_{ps}, was used, as suggested by Suzuki et al. (2010). The S_p value was also automatically recorded for all runs and is referred to as the *average value of the sound pressure* in Japan. In the analog signal processing system, a function for computing S_p was added. The system outputs the mean value of the enveloped raw data of the signal, which was computed to determine I_{ps}/I_{pv}, every 10 s, which is recorded as S_p by the data logger.

2.4.2. Acceleration sensor signal

The raw data of the signal obtained by the acceleration sensor corresponding to the sediment particle impacts were also registered in the experiment in the same manner as for the microphone signal. Similar to the microphone data processing, two parameters, I_{pv} and V_p, respectively corresponding to I_{ps} and V_p in the microphone signal processing, were calculated. Although V_p was computed in the same manner as for S_p via analog signal processing, I_{pv} was not computed for the acceleration signal because the performance of the data logger was not adequate for the computation. Therefore, I_{pv} was manually calculated along with the microphone signal, but the raw signal data were directly amplified by a factor of 2, 4, 16, 64, 256, and 1024 without converting the absolute values nor the enveloped signal data. Therefore, I_{pv} can be regarded as a kind of traditional impulse count made for the SPG system (Wyss et al., 2016b), which does not represent the number of detected particles. Subsequently, the value of I_{pv} for each amplification factor was defined as the number of times the amplified signal went above a predefined threshold of 2 V. Calculation of the I_{pv} parameters was simpler compared to that for the microphone signals because I_{ps} was computed by the data logger via analog signal processing; thus, it was difficult to completely reproduce and apply the analog processing to raw data of the acceleration signal on a PC.

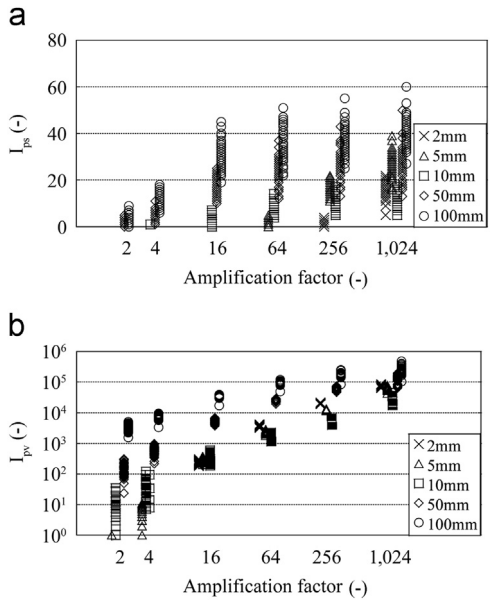

Fig. 9. Results of the number of pulses of each amplification factor ($V = 2.5$ m/s) for a) the microphone, and b) the acceleration sensor.

3. Results

3.1. Raw data of the signal

Fig. 7 (case 10, $V = 4.5$ m/s, $D_s = 100$ mm) and Fig. 8 (case 6, $V = 4.5$ m/s, $D_s = 2$ mm) show examples of the raw data of the signal recorded by the microphone and that recorded by the acceleration sensor, hereafter referred to as the microphone raw data of the signal and acceleration raw data of the signal, respectively. The top wave (a) is the microphone raw data of the signal, and the bottom wave (b) is the acceleration raw data of the signal. Both devices detected the impinging of gravel particles (Fig. 7). However, their forms are dissimilar. It was observed that the wavelength over time resulting from one gravel impact measured by the microphone is much longer than that measured by the acceleration sensor. Hence, the acceleration sensor has the advantage of avoiding the overlapping of waves when a large amount of sediment passes over it. It was also observed that the output voltages were sometimes saturated in the results of both sensors, especially for the acceleration sensor.

Fig. 8 clearly shows the difference between both devices when fine sediment hits the plate. Fig. 8a shows that the number of impulses registered by the microphone was limited because the impacts caused by sediment particles of $D_s = 2$ mm were so small that the produced signals were concealed under signal noise and the impacts were not detected. In contrast, the acceleration sensor detected several impulses apparently induced by the impact of sediment particles (Fig. 8b). Therefore, the microphone's limited sensitivity to small particles can be compensated for by using the vibration sensor.

3.2. The number of impulses

Fig. 9 shows the relation between the amplification factor and the number of impulses for $V = 2.5$ m/s (cases 1–5, Table 1), revealing that the number of impulses increases with increasing amplification. The reason is that more particle impacts exceeded the threshold voltage, and, thus, more particles were detected. The number of impulses of the acceleration sensor is many orders of magnitude higher than that of the microphone because of the different sensor characteristics (Section 2.4). The difference between the microphone raw data of the signal (Fig. 9a) and the acceleration raw data of the signal (Fig. 9b) is that the microphone cannot detect $D_s < 2$ mm, while the acceleration sensor can.

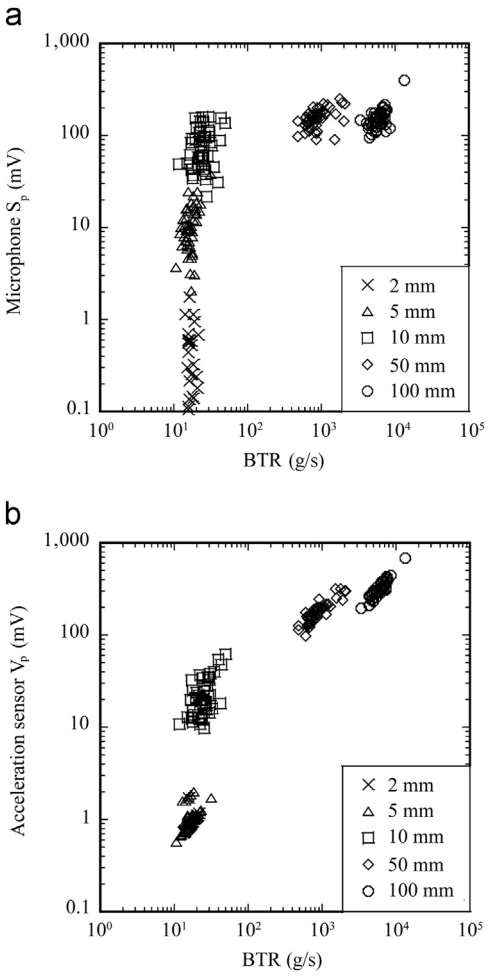

Fig. 10. a) Average value of sound pressure (S_p), and b) Average value of the acceleration sensor signal (V_p) versus the bedload transport rate (BTR) ($V = 2.5$ m/s).

3.3. Integrated value of output voltage

Fig. 10a and b show the values of S_p and V_p, respectively, versus the BTR for $V = 2.5$ m/s (cases 1–5). Here, the BTR is the weight used for each experiment and is divided by the duration T of each experiment. The duration T is defined as the time period between the first and last recorded signals resulting from particle impact in one experiment. Generally, the range of the BTR is limited because the test particles are fed manually. Data from the acceleration sensor (Fig. 10b) clearly indicate that the signals caused by sediment of sizes $D_s = 2$, 5, and 100 mm vary considerably between zero and several 100 mV, with V_p increasing with increasing diameter.

It should be considered that signal noise may also be shown in the figure. In particular, the S_p for a D_s of 2 mm is likely affected by noise. Indeed, the S_p for a D_s of 2 mm shows a scatter distribution ranging from 0.1 to 1.1 mV and is seemingly irrelevant with respect to the impact signal for particles with a D_s of 2 mm. Therefore, to achieve a reliable observation of small particles, a certain threshold should be determined to offset the signal noise based on the impact plate signal without any sediment transport (Rickenmann et al., 2014). Although the data of 5 and 10 mm gravel are distinguishable, those of 50 and 100 mm gravel are not,

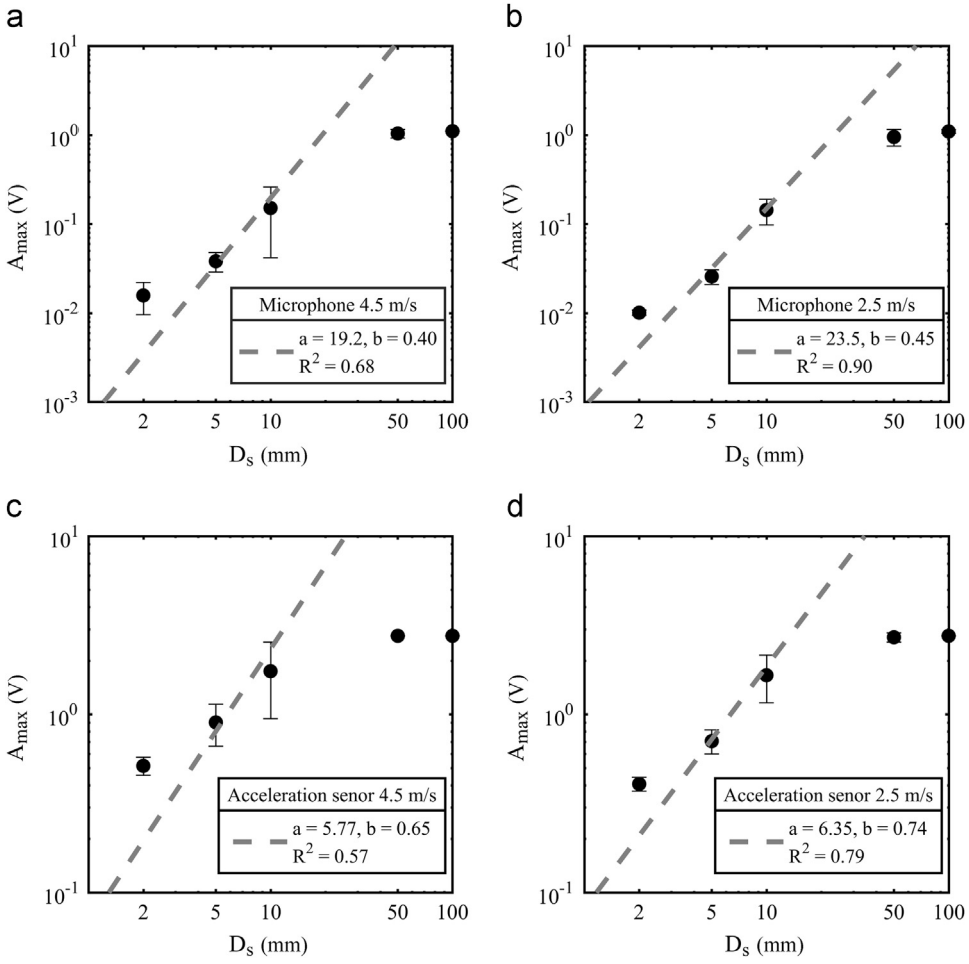

Fig. 11. Relation between the maximum amplitude (A_{max}) and the grain size (D_s). (a) microphone with $V = 4.5$ m/s, (b) microphone with $V = 2.5$ m/s, (c) acceleration sensor with $V = 4.5$ m/s and (d) acceleration sensor with $V = 2.5$ m/s.

as they are in the same energy range. It can be concluded that the waves overlapped when large sediment was transported. The microphone data (Fig. 10a) also show a positive correlation for $D_s = 10$, 50, and 100 mm, similar to the acceleration sensor data. However, the S_p values for $D_s = 2$ and 5 mm vary widely and show no correlation with the BTR. Thus, it is concluded that the microphone hardly detects fine sediment less than $D_s = 10$ mm.

3.4. Maximum amplitude

To estimate the largest particle size of the transported particles, the maximum amplitude, A_{max}, for each run is extracted from the microphone and acceleration raw data of the signal. It is already known that A_{max} is strongly correlated with the maximum grain size, which can be regarded as D_s in this study, since a uniform grain size was tested and is well fitted by a power law regression curve:

$$D_s = a \cdot A_{\max}{}^{b} \tag{1}$$

where a and b are constants (Rickenmann et al., 2014; Wyss et al., 2014). Fig. 11, which shows the relation between A_{max} and D_s with standard deviations, indicates that A_{max} increases as D_s increases. However, the standard deviation at $D_s = 50$ and 100 mm is almost zero for all results. According to the microphone and acceleration raw data of the signal, it is revealed that the output of both sensors became saturated when the microphone and the acceleration sensor received strong impacts, reaching 1.1 and 2.6 V, respectively. In the results, all values of A_{max} at $D_s = 100$ mm and more than half of the A_{max} values at $D_s = 50$ mm are saturated. Therefore, regression curves were calculated based on Eq. (1) without including the results for $D_s = 50$ and 100 mm. As shown in the figure, for both sensors, R^2 for $V = 2.5$ m/s is higher than R^2 for $V = 4.5$ m/s. This is likely related to the $V = 4.5$ m/s results exhibiting a higher standard deviation than those of $V = 2.5$ m/s because the higher flow velocity is more prone to turbulence, various particle transport modes (e.g., rolling, sliding, and saltation), and longer saltation length. The results also suggest that the A_{max} values obtained from the microphone signal are better fitted than the A_{max} values obtained from the acceleration sensor, as indicated by the R^2 value.

3.5. Detection rate

The detection rate, R_d, is defined as the number of detected impulses, I_{ps} (I_{pv} in the case of the acceleration sensor) divided by the number of particles used in one experiment, P_n, and it describes how much sediment is detected by the devices compared to the total sediment amount:

$$R_d = \frac{I_{ps}}{P_n} \tag{2}$$

Fig. 12 shows the relation between R_d and the amplification factor (for $V = 2.5$ m/s). In general, R_d increases with the amplification factor. The results of the microphone revealed that the values of R_d for $D_s = 2$ and 5 mm are low, hindering an accurate sediment transport rate estimation. In particular, the

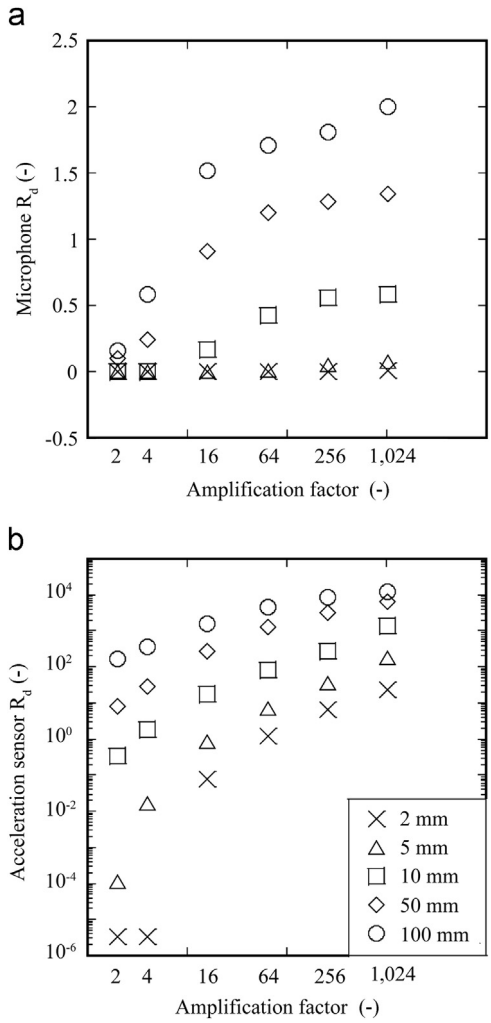

Fig. 12. Relation between the detection rate (R_d) and the amplification factor. (for V = 2.5 m/s) for a) the microphone, and b) the acceleration sensor.

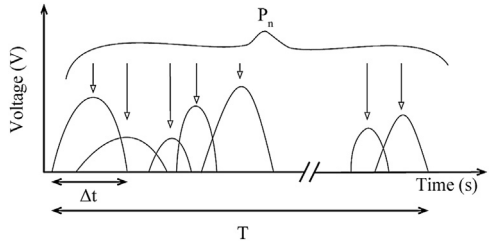

Fig. 13. Parameters which compose the saturation rate, R_s.

R_d values for D_s = 2 mm with 2-, 4-, 16-, and 64-fold amplification, for D_s = 5 mm with 2-, 4-, and 16-fold amplification, and for D_s = 10 mm with 2-fold amplification are zero. However, the detection rate for particles with D_s > 10 mm is good in general. Some R_d values are higher than one. This means that more than one impulse was generated by one particle impact because of the echo of that impact and the transport modes of rolling and sliding.

In Fig. 12b, the acceleration sensor R_d has a much larger range of values than that of the microphone R_d. This difference is attributed to the different methods used to process the signal. As noted in Section 2.4, I_{ps} was computed based on the enveloped raw data of the signal, whereas I_{pv} was computed based on the raw data. This difference resulted in a one to five orders of magnitude higher number of impulses compared to the number of impulses detected by the microphone (Fig. 9). The results of the acceleration sensor revealed that fine sediment with particle sizes less than 10 mm can be detected when the amplification factor is high. Moreover, focusing on an amplification factor larger than 4, R_d increases for all diameters.

Two parameters are proposed for characterizing R_d, namely, the saturation rate, R_s, and the hit rate, $P(L_p)$.

3.6. Saturation rate

As the BTR increases, the particle impacts tend to overlap with each other, which causes underestimation of the I_{ps} (I_{pv}); hence, a parameter that represents the bulk density is used to compute an accurate R_d value (Wyss et al., 2016b). The saturation rate, R_s, is the number of particles, P_n, that pass over the plate simultaneously, with the bulk density expressed as

$$R_s = \frac{P_n \cdot \Delta t}{T} \tag{3}$$

where, Δt = the average impact time of one particle hitting the plate. Δt was calculated based on additional flume experiments, in which a single particle was fed into the system to measure the impact duration caused by a single particle of D_s = 5, 10, 50, and 100 mm (ten runs for each grain size) (Fig. 13). It should be noted that P_n includes the particles that do not hit the plate; therefore, it is better to calculate R_s using the summed width of detected impulses instead of $P_n \cdot \Delta t$, similar to the overlapping probability presented in Wyss et al. (2016b). In this study, however, R_s was defined as Eq. 3 because the analog signal processing system outputs only I_{ps} and the width of each impulse cannot be determined affordably. Figs. 14 and 15 show the relation between R_d and R_s for amplification factors larger than 4 for D_s = 50 mm and V = 2.5 m/s. As R_s increases, R_d tends to decrease, presumably because of the increase in overlapped raw data of the signals resulting from interfering particles. Therefore, it can be concluded that particle impact saturation is one of the reasons for low R_d values. This tendency is confirmed for both devices, but the results for the acceleration sensor with the low amplification factor do not show the correlation well. The reason for this is that the impulses registered by the microphone tended to overlap because every wavelength was generally longer than those for the acceleration sensor, as mentioned in Section 3.1.

3.7. Hit rate

The particle saltation length directly affects R_d because longer saltation lengths cause a decrease in the hit rate for the plate. The saltation length, L_p, for supercritical flows can be calculated as follows (Auel et al., 2017a):

$$\frac{L_p}{D_s} = 2.3\left(\frac{\theta}{\theta_c} - 1\right)^{0.8} \tag{4}$$

where L_p = saltation length, θ = Shields' parameter, and θ_c = critical Shields' parameter (in this study, θ_c = 0.005 was chosen, in accordance with the study conducted by Auel et al. (2017a)).

Finally, the hit rate $P(L_p)$, which is based on the saltation length L_p, was defined as follows:

$$P(L_p) = \frac{B}{L_p} \tag{5}$$

where B = the plate length in the direction of the flow. The results obtained using Eq. (5) are shown in Fig. 16, where R_d is given as a function of $P(L_p)$. The data reveal that $P(L_p)$ increases with decreasing fluid velocity for both devices, as indicated by the arrows. According to the results of the microphone (Fig. 16a), at V = 4.5 m/s, particles tended to jump longer, and, hence, did not

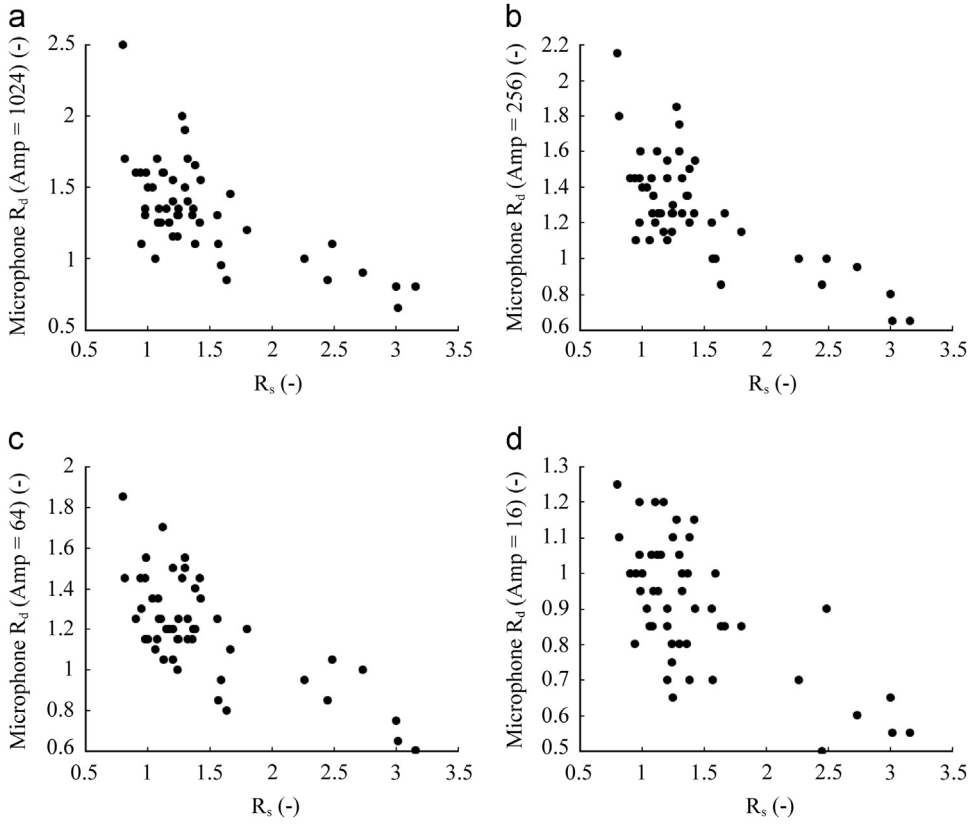

Fig. 14. The relation between the detection rate (R_d) and the saturation rate (R_s) of the plate microphone. (D_s = 50 mm, V = 2.5 m/s, amplification factor of (a) = 1024, (b) = 256, (c) = 64, and (d) = 16.

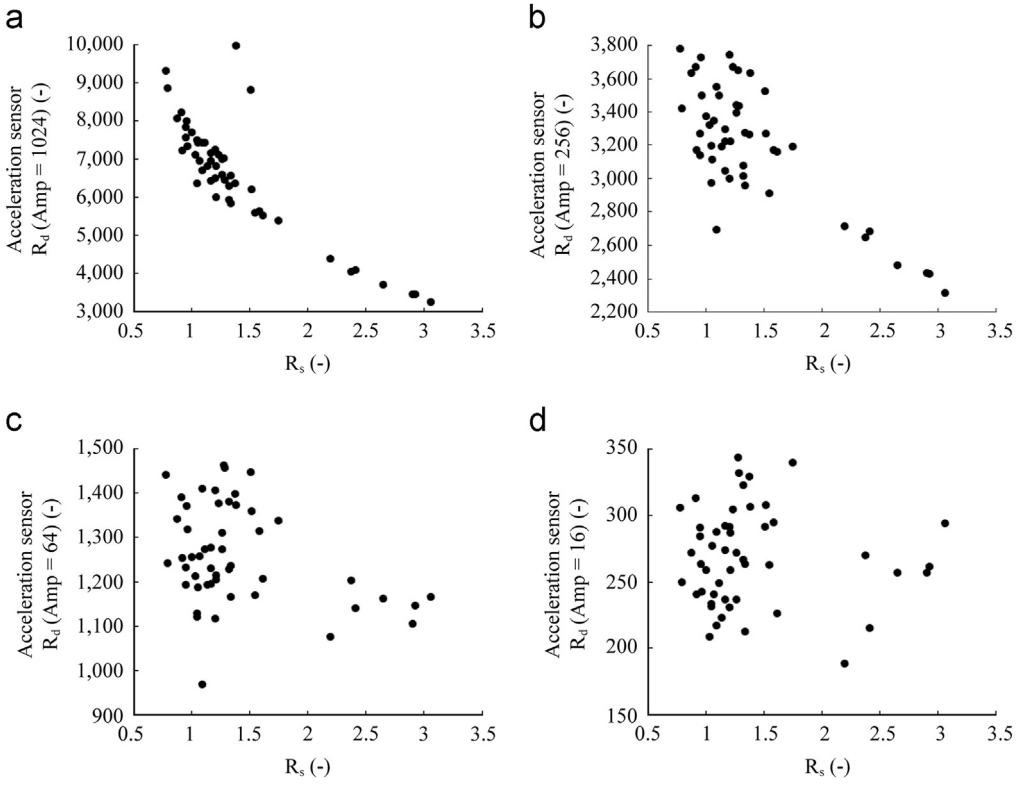

Fig. 15. The relation between the detection rate (R_d) and the saturation rate (R_s) of the acceleration sensor. (D_s = 50 mm, V = 2.5 m/s, amplification factor of (a) = 1024, (b) = 256, (c) = 64, and (d) = 16).

hit the plate often, whereas at $V = 2.5$ m/s, particles tended to roll or only jumped short distances, therefore, yielding a higher detection rate, R_d.

4. Discussion

Based on the laboratory calibration (more than 500 runs in total), one of the most important findings, as shown in Fig. 8, is that the acceleration sensor can detect particles with $D_s = 2$ mm. This result suggests that the impact plate successfully shows the desirable sensitivity to small particles at the $D_s > 2$ mm level while maintaining its robustness, although contrary to the authors' expectations, the microphone is found to exhibit less sensitivity than the acceleration sensor. However, Fig. 7a and b indicate that the signal of the acceleration sensor has many more peaks than that of the microphone, hence, inducing an over-estimation of the number of particles. Therefore, to monitor sediment with a wide range of grain sizes, both sensors need to be used for proper sediment analysis. Relatively large particles, which cause several impacts per particle because of their rotating and sliding modes, should be analyzed using microphone data. Small particles and saltating particles, on the other hand, which produce a single impact per a particle, can be analyzed using acceleration sensor data.

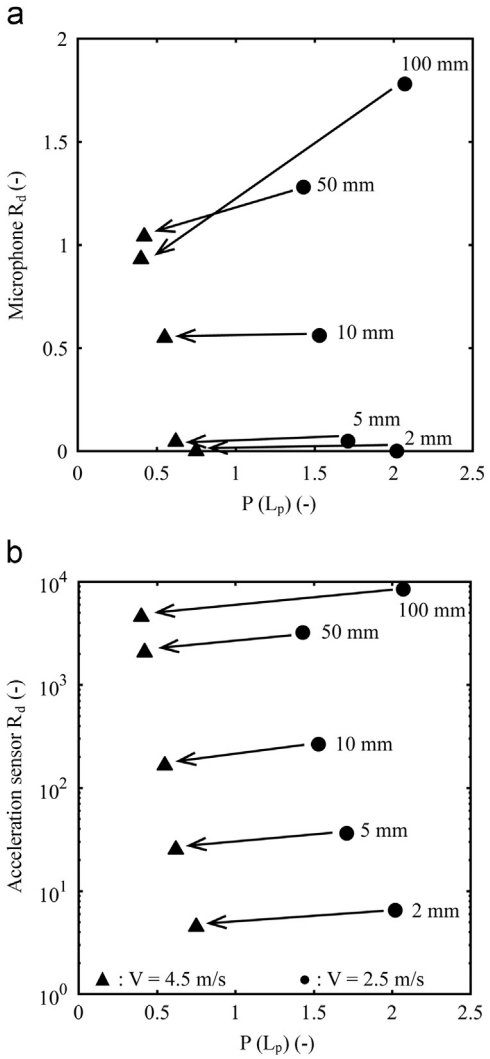

Fig. 16. The relation between the detection rate, R_d, and the hit rate, $P(L_p)$, for a) the microphone, and b) the acceleration sensor. Amplification factor = 256 times.

Although the simultaneous use of two sensors can improve the performance of sediment monitoring, distinguishing overlapping particle impacts might not easy. To disregard the influence of overlapping, R_s was introduced in this research. Another approach that can be used to address this problem is signal processing, which has been actively applied recently. In these studies, the characteristic frequency determined for single particle impacts was demonstrated to have a strong correlation with grain size (Møen et al., 2010; Wyss et al., 2016a). In particular, Belleudy et al. (2010) and Barrière et al. (2015) focused on signal processing and showed a considerable opportunity to exploit the raw data of signal analysis. Thus, the microphone and acceleration raw data of the signal were recorded as well as other parameters of the Koshibu SBT, in which impact plates are installed for monitoring sediment (Koshiba et al., 2016).

The SPG also uses a steel plate but has a geophone. The current research is in agreement with other studies on the SPG, revealing that the impact signals increase as the grain size or sediment volume increases (Wyss et al., 2014, 2016c). Therefore, the approach to measuring the sediment volume or grain size by counting the number of impulses ("packets" for the SPG) or signal amplitude, respectively, is similar to that for the SPG. The difference is that the impulses were computed with six levels of *Amp*. This parameter helps in analyzing the signals of a mixture of grain sizes. As in Fig. 12, R_d depends on the grain size; however, if R_d is calculated using only one *Amp* level, then R_d is not an efficient parameter for investigating the grain size when R_d has high variance. To solve this problem, the relation between R_d and *Amp* for each grain size seems to be useful. Theoretically, using R_d, the number of particles ($D_s = i$) that hit a plate, i.e. p_i, can be determined by solving the following equation:

$$I_j = \sum_i d_{ij} p_i \tag{6}$$

where, I_j is the observed I_{ps} or I_{pv} with $Amp = j$, $d_{ij} = R_d$ for $D_s = i$, and $Amp = j$. To confirm the effectiveness of Eq. 6, additional mixed grain size experiments with more recordings of the *Amp* value (i.e. smaller intervals) should be done.

The difference between the sensitivities of the impact plate and the SPG is implied. Although the SPG cannot detect fine sediment with diameters smaller than 2–4 cm, Fig. 8b indicates that the impact plate can detect particles of $D_s = 2$ mm. Meanwhile, there is an upper boundary of the detectable grain size for the acceleration sensor, as shown in Fig. 11c and d. In contrast, for the SPG, such an upper boundary has not been found in the literature, even when the grain size is larger than 100 mm (Wyss et al., 2016b). This difference might be caused by the difference between sensors, as both systems include a steel plate with the same dimensions.

Fig. 12 shows that I_{ps} and I_{pv} do not increase linearly with the amplification factor because of the increase in the sensitivity results when the impulse count is saturated (Mao et al., 2016; Mizuyama et al., 2010b). The newly introduced R_d measure is meaningful, as it directly connects the detected number of impulses and the actual amount of gravel impacting the plate. Therefore, if the R_d value for each grain size is calculated under the flow conditions, the actual amount of gravel can be calculated practically as the detected impulse number divided by R_d according to Eq. 6. As parameters representing the sediment transportation density and particle hop length, respectively, R_s and $P(L_p)$ are successfully found to have a correlation with R_d, as shown in Figs. 14–16. However, it is still difficult to accurately calculate these parameters. To obtain R_s, the number of particles is required, which is unknown for natural rivers; therefore, another method for calculating R_s is needed. In this case, turbidity can be used in

the Koshibu SBT. To compute $P(L_p)$ more accurately, other sediment particle modes of movement should be considered (Rickenmann et al., 2012; Tsakiris et al., 2014).

Impact plates are already installed at the outlet of the Koshibu SBT in the Nagano Prefecture in Japan and will be used from 2016 onward. Although the fundamental features of an impact plate are investigated in this study, it is indispensable to conduct calibration experiments at each field site where observations using the impact plates are planned because a device may exhibit behavior different from those observed in the flume experiments at the field sites (Beylich & Laute, 2014; Wyss et al., 2016c).

Moreover, in a SBT, the flow velocity reaches 10 m/s, which is much higher than that tested in this study. The authors' concern is that a higher flow velocity and a deeper flow depth will cause many more particles to jump over the plate. To mitigate this problem as much as possible, Auel and Boes (2011a) suggested utilizing plate inclination. In their study, it was concluded that a 10° SPG plate inclination increases the detection rate from 50% to 100% ($V = 7.4$ m/s). In response to this result, the eight SPGs deployed at the Solis SBT have the same 10° inclination angle (Hagmann et al., 2015). Accordingly, in the Koshibu SBT, one impact plate with a 10° inclination angle has been installed in addition to the five normal impact plates to compare their sensitivities.

5. Conclusions

Monitoring sediment transportation is necessary to operate and manage SBTs appropriately. In SBTs, however, robustness and the ability to detect a wide range of grain sizes under high flow velocity conditions are desired for monitoring systems. In this study, an impact-plate-type sediment monitoring system was introduced for monitoring sediment in SBTs. Approximately 500 runs of experiments were done to calibrate the impact plate with high flow velocity in a laboratory flume.

In the experiments, the acceleration sensor detected fine sediment with $D_s = 2$ mm, which cannot detected by the SPG or the JPM. However, the microphone could not detect sediment with $D_s = 2$ or 5 mm well. The different processes used to determine the attenuation time imply the efficiency of using both sensors simultaneously.

In addition to the raw data of the signals, two summary values, namely, I_{ps} and I_{pv}, were recorded. To acquire the actual number of particles from the number of impulses, the detection rate, R_d, was suggested. Making measurements using several amplification factors might improve the analysis of natural sediment that consists of particles of various grain sizes. Additional mixed grain size experiments with smaller intervals of amplification factors should be done to analyze the mixed size classes.

To calculate R_d for a given flow condition, the saturation rate, R_s, and plate impact rate, $P(L_p)$, were proposed, and high correlation between R_d and both parameters was found. Although more experiments are required to quantify R_d, R_s, and $P(L_p)$, these parameters might be field-dependent. Therefore, several field calibrations at the Koshibu SBT, in which a predefined amount of sediment is artificially placed inside the tunnel and then flushed out, are being done.

Acknowledgments

The authors acknowledge the support of VAW of ETH Zurich for excellent collaboration during the experiments. Many thanks also go to the Ministry of Land, Infrastructure, Transport, and Tourism (MLIT) for fruitful discussion. This work was also supported by JSPS KAKENHI Grant number 26257304 and by the regional research project of river and sediment management technology development by MLIT (H26-85-4). The second author acknowledges the support of the Japan Society for the Promotion of Science (P14776). The also thank Dieter Rickenmann, an anonymous reviewer, the Associate editors Jochen Aberle, and Charles Steven Melching for their comments which further helped to improve the manuscript.

References

Auel, C. (2014). *Flow characteristics, particle motion and invert abrasion in sediment bypass tunnels. (Doctoral dissertation)*. ETH Zurich, Switzerland. ⟨http://dx.doi.org/10.3929/ethz-a-010243883⟩.

Auel, C., Albayrak, I., Sumi, T., & Boes, R. M. (2017a). Sediment transport in high-speed flows over a fixed bed: 1. *Particle Dynamics Earth Surface Processes and Landforms*. , http://dx.doi.org/10.1002/esp.4128.

Auel, C., & Boes, R. M. (2011a). Sediment bypass tunnel design - Hydraulic model tests. In *Proceedings of the Hydro 2011- practical solutions for a sustainable future*, *29*(3). Prague, Czech Republic: Aqua-Media International Ltd.

Auel, C., & Boes, R. M. (2011b). Sediment bypass tunnel design - Review and outlook. In A. J. Schleiss & R. M. Boes (Eds.), *ICOLD symposium, dams under changing challenge. Proceedings of the 79th annual meeting*. Lucerne (pp. 403–412). London: Taylor & Francis.

Auel, C., Boes, R. M., & Sumi, T. (2016a). Abrasion prediction at Asahi sediment bypass tunnel based on Ishibashi's formula. *Journal of Applied Water Engineering and Research*. http://dxdoi.org/10.1080/23249676.2016.1265470.

Auel, C., Kantoush, S. A., & Sumi, T. (2016b). Positive effects of reservoir sedimentation management on reservoir life – examples from Japan. *In Proceedings of the 84th annual meeting of ICOLD* (pp. 4–11 - 4-20). Johannesburg, South Africa.

Auel, C., Kobayashi, S., Takemon, Y., & Sumi, T. (2017b). Effects of sediment bypass tunnels on grain size distribution and benthic habitats in regulated rivers. *International Journal of River Basin Management*, *15*(4), 433–444. http://dx.doi.org/10.1080/15715124.2017.1360320.

Barrière, J., Krein, A., Oth, A., & Schenkluhn, R. (2015). An advanced signal processing technique for deriving grain size information of bedload transport from impact plate vibration measurements. *Earth Surface Processes and Landforms*, *40*(7), 913–924.

Baumer, A., & Radogna, R. (2015). Rehabilitation of the Palagnedra sediment bypass tunnel (2011–2013). In: R. M. Boes (Ed.), *Proceedings international workshop on sediment bypass tunnels* (pp. 235–245). ETH Zurich, Switzerland: VAW-Mitteilung 232.

Belleudy, P., Valette, A., & Graff, B. (2010). Passive hydrophone monitoring of bedload in river beds: First trials of signal spectral analyses In: J. R. Gray, J. B. Laronne, & J. D. G. Marr (Eds.), *Bedload-surrogate monitoring technologies* (pp. 67–84). U.S. Geological Survey Scientific Investigations 2010-5091.

Beylich, A. A., & Laute, K. (2014). Combining impact sensor field and laboratory flume measurements with other techniques for studying fluvial bedload transport in steep mountain streams. *Geomorphology*, *218*, 72–87.

Bunte, K., Abt, S. R., Potyondy, J. P., & Ryan, S. E. (2004). Measurement of coarse gravel and cobble transport using portable bedload traps. *Journal of Hydraulic Engineering*, *130*(9), 879–893.

Facchini, M., Siviglia, A., & Boes, R. M. (2015). Downstream morphological impact of a sediment bypass tunnel - Preliminary results and forthcoming actions. In R. M. Boes (Ed.) *Proceedings of the international workshop on sediment bypass tunnels* (pp. 137–146). VAW-Mitteilung 232, ETH Zurich, Switzerland.

Goto, K., Itoh, T., Nagayama, T., Kasai, M., & Marutani, T. (2014). Experimental and theoretical tools for estimating bedload transport using a Japanese pipe hydrophone. *International Journal of Erosion Control Engineering*, *7*(4), 101–110.

Gray, J. R., Laronne, J. B., & Marr, J. D. (2010). Bedload-surrogate monitoring technologies. *U.S. Geological Survey Scientific Investigations Report 2010–5091*.

Hagmann, M., Albayrak, I., & Boes, R. M. (2015). Field research: Invert material resistance and sediment transport measurements. In R. M. Boes (Ed.) *Proceedings of the international workshop on sediment bypass tunnels* (pp. 123–135). VAW-Mitteilung 232, ETH Zurich, Switzerland.

Helley, E. J., & Smith, W. (1971). Development and calibration of a pressure-difference bedload sampler. *U.S. Geological Survey, Open-File Report, 73-108*.

Ishibashi, T. (1983). Hydraulic study on protection for erosion of sediment flush equipments of dams. *Civil Society Process*, *334*(6), 103–112 (In Japanese).

Jacobs, F., & Hagmann, M. (2015). Sediment bypass tunnel Runcahez: Invert abrasion 1995–2014. In R. M. Boes (Ed.), *Proceedings of the international workshop on sediment bypass tunnels* (pp. 211–221). VAW-Mitteilung 232, ETH Zurich, Switzerland.

Kantoush, S. A., Sumi, T., & Murasaki, M. (2011). Evaluation of sediment bypass efficiency by flow field and sediment concentration monitoring techniques. Journal of Japan Society of Civil Engineers. *Ser B1 (Hydraulic Engineering)*, *67*(4), 169–174.

Koshiba, T., Sumi, T., Tsutsumi, D., Kantoush, S. A., & Auel, C. (2016). Development of a bedload transport measuring system for sediment bypass tunnels in Japan. *In*

Proceedings of the 84th annual meeting of ICOLD (pp. 4–49 - 4-58). Johannesburg, South Africa.

Mao, L., Carrillo, R., Escauriaza, C., & Iroume, A. (2016). Flume and field-based calibration of surrogate sensors for monitoring bedload transport. *Geomorphology*, *253*, 10–21.

Mizuyama, T., Fujita, M., & Nonaka, M. (2003). Measurement of bedload with the use of hydrophones in mountain torrents. In *Proceedings of the workshop erosion and sediment transport measurement in rivers: Technological and methodological advances* (pp. 222–227). Oslo, Norway.

Mizuyama, T., Laronne, J. B., Nonaka, M., Sawada, T., Satofuka, Y., Matsuoka, M., & Yamashita, S. (2010a). Calibration of a passive acoustic bedload monitoring system in Japanese mountain rivers In: J. R. Gray, J. B. Laronne, & J. D. G. Marr (Eds.), *Bedload-surrogate monitoring technologies* (pp. 296–318). U.S. Geological Survey Scientific Investigations 2010-5091.

Mizuyama, T., Matsuoka, M., & Nonaka, M. (2008). Bedload measurement by acoustic energy with hydrophone for high sediment transport rate. *Journal of the Japan Society of Erosion Control Engineering*, *61*(1), 35–38 (In Japanese).

Mizuyama, T., Oda, A., Laronne, J. B., Nonaka, M., & Matsuoka, M. (2010b). Laboratory tests of a Japanese pipe geophone for continuous acoustic monitoring of coarse bedload In: J. R. Gray, J. B. Laronne, & J. D. G. Marr (Eds.), *Bedload-surrogate monitoring technologies* (pp. 319–335). U.S. Geological Survey Scientific Investigations 2010-5091.

Møen, K. M., Bogen, J., Zuta, J. F., Ade, P. K., & Esbensen, K. (2010). Bedload measurement in rivers using passive acoustic sensors In: J. R. Gray, J. B. Laronne, & J. D.G. Marr (Eds.), *Bedload-surrogate monitoring technologies* (pp. 336–351). U.S. Geological Survey Scientific Investigations 2010-5091.

Nakajima, H., Otsubo, Y., & Omoto, Y. (2015). Abrasion and corrective measures of a sediment bypass system at Asahi Dam. In R. M. Boes (Ed.), *Proceedings of the international workshop on sediment bypass tunnels* (pp. 21–32). VAW-Mitteilung 232, ETH Zurich, Switzerland.

Reid, I., Layman, J. T., & Frostick, L. E. (1980). The continuous measurement of bedload discharge. *Journal of Hydraulic Research*, *18*(3), 243–249.

Reid, S. C., Lane, S. N., Berney, J. M., & Holden, J. (2007). The timing and magnitude of coarse sediment transport events within an upland, temperate gravel-bed river. *Geomorphology*, *83*(1), 152–182.

Rickenmann, D. (2017a). Bedload transport measurements with geophones and other passive acoustic methods. *Journal of Hydraulic Engineering*, *143*(6), 03117004.

Rickenmann, D. (2017b). Bedload transport measurements with geophones, hydrophones and underwater microphones (passive acoustic methods) In: D. Tsutsumi, & J. B. Laronne (Eds.), *Gravel bed rivers and disasters* (pp. 185–208). Chichester: U.K.: Wiley.

Rickenmann, D., Antoniazza, G., Wyss, C. R., Fritschi, B., & Boss, S. (2017). Bedload transport monitoring with acoustic sensors in the Swiss Albula mountain river. *In Proceedings of the international association of hydrological sciences*, *375*, 5-10.

Rickenmann, D., & McArdell, B. W. (2007). Continuous measurement of sediment transport in the Erlenbach stream using piezoelectric bedload impact sensors. *Earth Surface Processes and Landforms*, *32*(9), 1362–1378.

Rickenmann, D., Turowski, J. M., Fritschi, B., Klaiber, A., & Ludwig, A. (2012). Bedload transport measurements at the Erlenbach Stream with geophones and automated basket samplers. *Earth Surface Processes and Landforms*, *37*(9), 1000–1011.

Rickenmann, D., Turowski, J. M., Fritschi, B., Wyss, C., Laronne, J., Barzilai, R., & Habersack, H. (2014). Bedload transport measurements with impact plate geophones: Comparison of sensor calibration in different gravel-bed streams. *Earth Surface Processes and Landforms*, *39*(7), 928–942.

Roth, D. L., Brodsky, E. E., Finnegan, N. J., Rickenmann, D., Turowski, J. M., & Badoux, A. (2016). Bed load sediment transport inferred from seismic signals near a river. *Journal of Geophysical Research: Earth Surface*, *121*(4), 725–747.

Schwalt, M., & Hager, W. H. (1992). Die Strahlbox (The jetbox). *Schweizer Ingenieur und Architekt*, *110*(27/28), 547–549 (*In German*).

Sumi, T., Okano, M., & Takata, Y. (2004). Reservoir sedimentation management with bypass tunnels in Japan. *In Proceedings of the 9th international symposium on river sedimentation* (pp. 1036–1043). Yichang, China.

Suzuki, T., Mizuno, H., Osanai, N., Hirasawa, R., & Hasegawa, Y. (2010). Basic study on sediment rate measurement with a hydrophone on the basis of sound pressure data. *Journal of the Japan Society of Erosion Control Engineering*, *62*(5), 18–26 (*In Japanese*).

Taniguchi, S., Itakura, Y., Miyamoto, K., & Kurihara, J. (1992). A new acoustic sensor for sediment discharge measurement (IAHS Publication 210). In: J. Bogen, D. E. Walling, & T. J. Day (Eds.), *Erosion and sediment transport monitoring programs in river basins* (pp. 135–142). Wallingford: International Association of Hydrological Sciences.

Tsakiris, A. G., Papanicolaou, A. T. N., & Lauth, T. J. (2014). Signature of bedload particle transport mode in the acoustic signal of a geophone. *Journal of Hydraulic Research*, *52*(2), 185–204.

Tsutsumi, D., Hirasawa, R., Mizuyama, T., Shida, M., & Fujita, M. (2010). *Bed load observation in a mountainous watershed by hydrophone equipments* (pp. 537–543)Annuals of Disaster Prevention Research Institute, Kyoto University (*In Japanese*).

Wyss, C. R., Rickenmann, D., Fritschi, B., Turowski, J. M., Weitbrecht, V., & Boes, R. M. (2014). Bedload grain size estimation from the indirect monitoring of bedload transport with Swiss plate geophones at the Erlenbach Stream In: A. J. Schleiss, G. De Cesare, M. J. Franca, & M. Plister (Eds.), *River flow* (pp. 1907–1912). London: Taylor & Francis Group.

Wyss, C. R., Rickenmann, D., Fritschi, B., Turowski, J. M., Weitbrecht, V., & Boes, R. M. (2016a). Laboratory flume experiments with the Swiss plate geophone bed load monitoring system: 1. Impulse counts and particle size identification. *Water Resources Research*, *52*(10), 7744–7759.

Wyss, C. R., Rickenmann, D., Fritschi, B., Turowski, J. M., Weitbrecht, V., & Boes, R. M. (2016b). Measuring bed load transport rates by grain-size fraction using the Swiss plate geophone signal at the Erlenbach. *Journal of Hydraulic Engineering*, *142*(5), 04016003.

Wyss, C. R., Rickenmann, D., Fritschi, B., Turowski, J. M., Weitbrecht, V., Travaglini, E., & Boes, R. M. (2016c). Laboratory flume experiments with the Swiss plate geophone bed load monitoring system: 2. Application to field sites with direct bed load samples. *Water Resources Research*, *52*(10), 7760–7778.